

## Modelling of a Magnetostrictive Torque Sensor

Vasilios Tsiantos<sup>1</sup>, Vasilios Karagiannis<sup>2</sup>, Aphrodite Ktena<sup>2</sup>, Christos Manasis<sup>2,a</sup>, Onoufrios Ladoukakis<sup>2</sup>, Charalambos Elias<sup>2</sup>, Evangelos Hristoforou<sup>3</sup> and Polyxeni Vourna<sup>3</sup>

<sup>1</sup>Electrical Engineering Department, TEI of Eastern Macedonia and Thrace, Kavala, Greece

<sup>2</sup>Electrical Engineering Department, TEI of Sterea Ellada, Psachna, Greece

<sup>3</sup>School of Mining and Metallurgical Engineering, National Technical University of Athens, Athens, Greece

**Abstract**— Existing magnetostrictive torque sensor designs typically measure the rotation of the saturation magnetization under an applied torque and their theoretical treatment revolves around the minimization of the free energy equation adapted according to the assumptions considered valid in each design. In the torque measurement design discussed in this paper, Ni-rich NiFe films have been electrodeposited on cylindrical austenitic steel rods. Contrary to existing designs, the excitation field is applied along the axial direction and is low enough to ensure that the resulting magnetization along the same direction remains in the linear region of the  $M(H)$  characteristic. Assuming homogeneous magnetization, positive magnetostriction constant  $\lambda$ , negligible hysteresis and demagnetizing fields, torque  $T$  may be expressed in terms of an effective uniaxial anisotropy constant  $K_u$  around  $45^\circ$  to the axial direction. It is shown, that for the proposed arrangement, the resulting  $M$  is the linear superposition of the effect of a torque-induced effective field and the excitation field, the applied field accounts for the vertical offset of the magnetization response and the applied torque increases the slope of the  $M(H)$  characteristic.

### 1. Introduction

The use of magnetostriction in torque sensing has resulted in several interesting designs, their advantage being the inherent contactless measurement: pre-strained amorphous FeSiB magnetostrictive ribbons have been glued around the rotating shaft with excitation and sensing coils placed around the rotating shaft to measure the change of the axial permeability due to the applied torque [1]; a magnetostrictive CoSiB ribbon attached around the shaft has been used with a yoke-type arrangement for the excitation and sensing elements [2,3] in order to pick up the changes in the flux emanating from the ribbon due to the surface stresses induced by the torque; excitation and pick up coil arrangements have been placed around a rotating shaft made of magnetostrictive steel [4] but the arrangement is complicated and the measurement suffers from the high hysteresis of this type of steel; the axial stress-induced magnetization component on a circumferentially pre-magnetized magnetostrictive ring and attached firmly around the rotating shaft [5,6,7] has been measured.

The magnetostrictive torque sensing arrangement presented in this work, utilizes NiFe films, of several microns, electrodeposited on nonmagnetic steel shafts,

<sup>a</sup> Corresponding author: manasis@teiste.gr

thus avoiding adhesives or other means of attaching the sensing element on the shaft (Fig. 1).

Static torque is applied on the free end of the shaft. The NiFe film lies inside a solenoid and is magnetized along the axial direction [4] which is also the measurement direction (Fig. 2). A sensing coil wound around the sensing element picks up the changes in axial susceptibility due to the torque induced stress field.

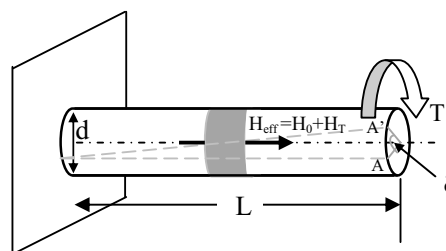


**Figure 1** The torque sensing arrangement: The effective field  $H_{eff}$  along the axial direction is the sum of the applied field  $H_0$  and the effective torque induced field  $H_T$

This arrangement, contrary to other magnetostrictive torque sensors proposed in the literature [1,7] (i) does not measure the rotation of the magnetization under the effect of the applied torque but the change in

differential susceptibility in the direction of the applied field, under the effect of the torque-induced effective field,  $H_{eff}$  and (ii) must not be saturated but instead it should be operated in the quasi-linear region of the NiFe hysteresis curve under low applied fields.

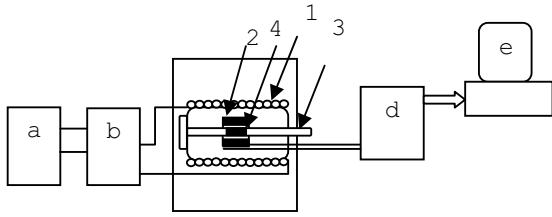


**Figure 2** - Experimental setup (a) sine wave generator, (b) amplifier, (c) magnetometer: (1) excitation coil, (2) sensing coil, (3) cylindrical specimen, (4) NiFe magnetostrictive film, (d) data acquisition card, (e) computer

It must be noted, that the proposed sensing arrangement may also be used directly in shafts made of magnetostrictive materials, such as low carbon and martensitic steels common in boat shafts, as long as hysteresis is compensated for by an appropriate hysteresis model. The sample preparation, measurement procedure and experimental results are briefly overviewed in the following section while the rest of the article presents the modelling of the proposed arrangement as proof of concept and optimization tool.

## 2. Materials and methods

0.10 m long cylindrical NiFe films were electrodeposited on non magnetic austenitic stainless steel 316L (USA AISI) shafts of 10mm diameter and 0.30 m long [8]. A sinusoidal field is generated inside a long solenoid at the centre of which, where the field is expected to be homogeneous, the electroplated shaft is placed. Compensation coils are wound in series opposition to the sensing coil. Static torque is applied by means of suspended standard weights at the free end of a 0.50 m arm fitted perpendicular to the shaft. Two series of measurements have been carried out with (i) increasing torque,  $T$ , at constant excitation field magnitude,  $H_0$  (ii) increasing  $H_0$  at constant  $T$ . The voltage waveform induced at the ends of a pickup coil placed around the centre of the NiFe sample is measured via a NI 6251 card. Following Faraday's law of induction, the output voltage,  $V(t)$ , is proportional to the sample's differential susceptibility  $\chi_{diff}$  (Fig. 2). Figs. 3-4 show the measured peak value of the output voltage  $V_{peak}$  for a Ni<sub>60</sub>Fe<sub>40</sub> sample. The field axis in Fig. 4 is in arbitrary units (au).  $V_{peak}$  is proportional to the maximum slope of the hysteresis curve  $M(H)$  for this sample:

$$V_{peak} \propto \chi_{diff}(H_0) = \frac{dM}{dH} \Big|_{H_0} \quad (1)$$

where  $H_0$  is the applied field magnitude which sets the operating point in the linear region of the  $M(H)$  curve. Hysteresis is assumed negligible for this type of material.

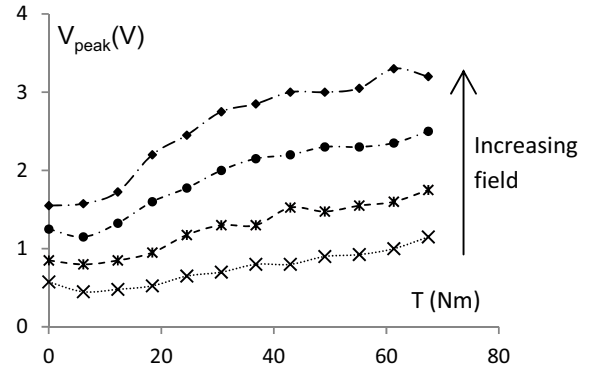


**Figure 3** – Output voltage peak,  $V_{peak}$ , vs torque  $T$  at increasing applied fields.

When torque  $T$  is applied, the effective field  $H_{eff}$  acting on the axial differential susceptibility measured,  $\chi_{diff}(H_{eff})$ , is the sum of the applied field magnitude  $H_0$  and a torque induced axial component  $H_T$ :

$$H_{eff} = H_0 + H_T \quad (2)$$

For an applied bias field  $H_0$  such that the resulting  $M$  is in the linear region of the  $M(H)$  characteristic, a linear dependence, as the one shown in Fig. 4, may be assumed:  $\chi_{diff} = aH_{eff}$ , where  $a$  is the slope of the differential susceptibility field dependence. Then, the resulting  $V_{peak}$  increases almost linearly with torque  $T$  (Fig. 3) for a given applied field  $H_0$ :

$$V_{peak}(T) = V(H_0) + k_1 T \quad (3)$$

where  $k_1$  is a constant related to the magnetization curve and reflecting the sensitivity of the film at the given operating point.

At constant  $T$ :

$$V_{peak}(H) = a' H_{eff} \quad (4)$$

$a'$  is the slope of the  $\chi_{diff}(H_{eff})$  characteristic for the given  $T$  (Fig. 4):

$$a' = a + k_2 H_T \quad (5)$$

where  $k_2$  is a constant.

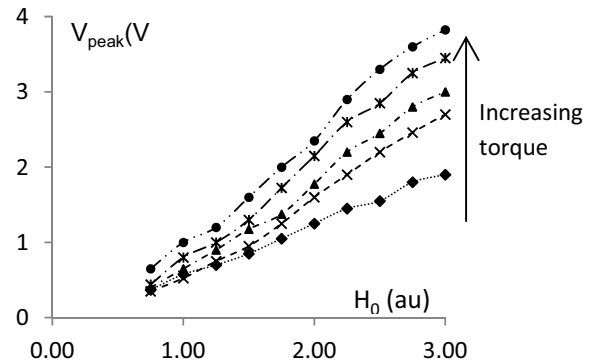


**Figure 4**– Output voltage peak,  $V_{peak}$ , vs applied field  $H_0$  (arbitrary units) at increasing torque levels.

### 3. Sensor modelling

In the case of a shaft under torque  $T$  (Fig.1) with modulus of rigidity  $G$ , the surface shear strain  $\varepsilon$  is proportional to shaft's diameter  $d$  and the displacement angle  $\delta$  and inversely proportional to the shaft's length  $L$ :

$$\varepsilon = \frac{d\delta}{2L} \quad (6)$$

The surface shear stress  $\sigma$  is proportional to the strain  $\varepsilon$

$$\sigma = G\varepsilon = G \frac{d\delta}{2L} \quad (7)$$

Torque  $T$  is proportional to  $\sigma$  and the polar moment of inertia of the shaft's cross section  $J$  and inversely proportional to the diameter  $d$ :

$$T = \frac{2}{d} \sigma J \quad (8)$$

Hence, stress and torque are related via:

$$\sigma = \frac{16T}{\pi d^3} \quad (9)$$

The torque related orthogonal stresses  $\sigma$ , as given by (9), induce a uniaxial anisotropy  $K_u$  at an angle  $\phi$ , which is close to  $45^\circ$  [1]:

$$K_u = \frac{3}{2} \lambda \sigma = \frac{48}{\pi d^3} \frac{G_{NiFe}}{G_{steel}} \lambda T \quad (10)$$

where  $\lambda$  is the magnetostrictive constant of the sensing element,  $G_{NiFe}$  is the modulus of rigidity of the NiFe film deposited on the shaft and  $G_{steel}$  is the modulus of rigidity of the steel substrate.

The anisotropy energy term is then written as:

$$E_K = K_u \sin^2 \theta \quad (11)$$

where  $\theta$  is the angle of  $M$  with the induced easy axis.

The demagnetizing energy term can be ignored in this setup with no loss of generality because the NiFe film is much shorter than the excitation solenoid and immersed at the center of the magnetizing field while the pickup coil is shorter than the NiFe film and positioned around the center of the film. The only other contributing energy term is the applied field energy  $E_H$ :

$$E_H = -\mathbf{M} \cdot \mathbf{H}_0 = -MH_0 \cos(\varphi - \theta) \quad (12)$$

where  $\phi$  is the angle of the applied field  $H_0$  with the induced easy axis.

The minimization of the total energy with respect to  $\theta$  yields:

$$\frac{dE}{d\theta} = -MH \sin(\varphi - \theta) + 2K_u \sin \theta \cos \theta \quad (13)$$

the solution of which corresponds to the coherent rotation mechanism described by the Stoner-Wohlfarth model.

Next, we define the effective field  $H_{eff}$  as the field that satisfies the relationship:

$$\begin{aligned} -MH_0 \sin(\varphi - \theta) + 2K_u \sin \theta \cos \theta = \\ -MH_{eff} \sin(\varphi - \theta) \end{aligned} \quad (14)$$

Given (2), the torque induced field,  $H_T$ , is deduced from (14):

$$H_T = \frac{K_u \sin 2\theta}{M(\cos \varphi \sin \theta - \sin \varphi \cos \theta)} \quad (15)$$

$H_T$  is proportional to the torque induced anisotropy  $K_u$  and hence to  $T$ , as given by (10), and it depends on the angle  $\phi$  that  $H_0$  forms with the induced easy axis. At  $\phi = 0$ , ie when  $H_0$  is applied at  $0^\circ$  to the easy axis,  $H_T$  is maximum, which is consistent with results on other sensor designs based on the maximum rotation of  $M$ .

In the absence of torque  $T$ ,  $H_T = 0$ , and  $H_{eff} = H_0$ . In the proposed setup,  $\varphi = -45^\circ$ , ie  $H_0$  is applied along the axial direction of the rod and

$$H_{eff} = H_0 + \frac{K_u \sin 2\theta}{\frac{\sqrt{2}}{2} M (\cos \theta - \sin \theta)} \quad (16)$$

The dependence of  $H_T$  on torque  $T$  and the magnetization angle  $\theta$  is shown in Fig. 5 for various angles  $\phi$  of the applied field  $H_0$  with the torque induced easy axis.

The calculated results shown refer to a  $Ni_{60}Fe_{40}$  sample with  $\lambda = +2.5 \times 10^{-5}$ . The moduli of rigidity are taken to be  $G_{steel} = 90 \times 10^9$  N/m<sup>2</sup> and  $G_{NiFe} = 70 \times 10^9$  N/m<sup>2</sup>.

In agreement with the analysis of the experimental data in the previous section, the torque induced field  $H_T$  varies proportionally with the torque  $T$ . Angle  $\theta$  controls the slope of the curve and reflects the balance between the applied field  $E_H$ , and the torque induced anisotropy energy  $E_K$ .

Figure 5 shows the computed dependence of torque induced field  $H_T$  on the applied torque for two different applied field angles  $\phi$ .

The proposed modeling approach describes adequately the experimental results. The simplifying assumptions underlying the solution account for the deviations of the experimental results from the linear behavior.

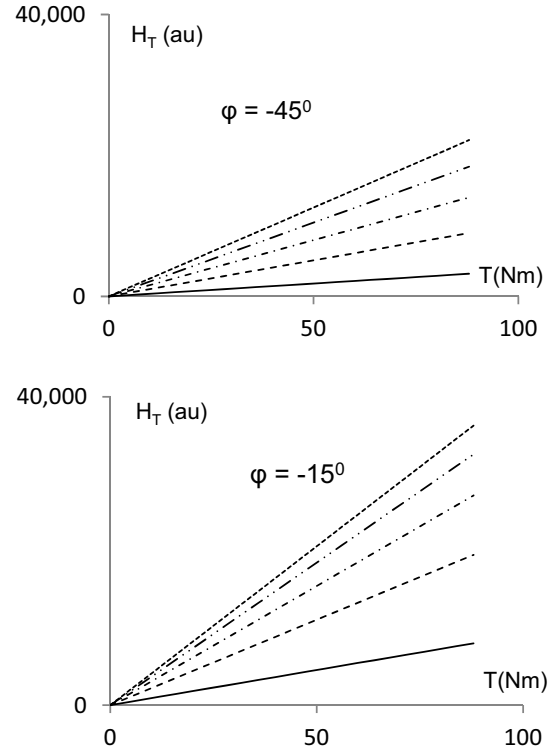


**Figure 5** – The dependence of torque induced field  $H_T$  on applied torque  $T$  for increasing values of  $\theta$  (solid line corresponds to smallest angle value) and  $\varphi = -45^\circ, -15^\circ$

#### 4. Conclusions

Our theoretical treatment aims in explaining the experimental observations of a torque sensor arrangement which differs from existing designs in the following points: (i) the magnetostrictive film is electrodeposited on the shaft thus avoiding adhesives or other invasive attachment methods (ii) the excitation and the readout of the sensor are both along the axial direction with no need for preprocessing of the magnetic properties of the sensor (iii) the sensor is operated in the linear part of the  $M(H)$  away from saturation and therefore low fields are needed (iv) the output does not depend on the readout of the rotation of the magnetization but on the superposition of a torque induced field and the applied field, along the axial direction. The output voltage is proportional to the applied torque. The applied field bias sets the operating point and accounts for the vertical offset of the output voltage. The arrangement can also be used directly on magnetostrictive shafts, as long as hysteresis is compensated.

#### Acknowledgement

This research has been co-financed by the European Union (European Social Fund – ESF) and Greek national funds through the Operational Program "Education and Lifelong Learning" of the National Strategic Reference Framework (NSRF) - Research Funding Program: ARCHIMEDES III. Investing in knowledge society through the European Social Fund.

#### References

1. K. Harada, I. Sasada, T. Kawajiri, M. Inoue, IEEE Transactions on Magnetics, 18 (6) (1982) 1767-1769
2. Pirmin Rombach, Werner Langheinrich, Sensors and Actuators A, 46 (1995) 294-297
3. Frank Umbach, Heinrich Acker, Johannes von Kluge, Werner Langheinrich, Mechatronics, 12 (2002) 1023–1033
4. Hiroyuki Wakiwaka, Muneo Mitamura, Sensors and Actuators A, 91 (2001) 103-106
5. I.J. Garshelis, IEEE Transactions on Magnetics, 28 (5) (1992) 2202—2204
6. F.E. Pinkerton, J.F. Herbst, C.H. Olk, M.S. Meyer, J.J. Moleski, Journal of Magnetism and Magnetic Materials, 241 (2002) 162–172
7. Herbst, J. F., and F. E. Pinkerton, Journal of Magnetism and Magnetic Materials, 176(2) (1997) 183-196
8. Ktena Aphrodite, Manasis Christos, Tsakiridis Petros, Sensor Letters, 11 (2013) 184–186